

MOL # 115303

1 **A small-molecule compound selectively activates K2P channel TASK-3 by**  
2 **acting at two distant clusters of residues**

3 Fuyun Tian<sup>1,2</sup>, Yunguang Qiu<sup>1,2</sup>, Xi Lan<sup>1,2</sup>, Min Li<sup>3</sup>, Huaiyu Yang<sup>4</sup> and Zhaobing Gao<sup>1,2\*</sup>

4 *<sup>1</sup>CAS Key Laboratory of Receptor Research, State Key Laboratory of Drug Research,*  
5 *Shanghai Institute of Materia Medica, Chinese Academy of Sciences, Shanghai, 201203,*  
6 *China. <sup>2</sup>University of Chinese Academy of Sciences, 19A Yuquan Road, Beijing, 100049,*  
7 *China. <sup>3</sup> Department of Neuroscience, High Throughput Biology Center and Johns Hopkins*  
8 *Ion Channel Center, School of Medicine, Johns Hopkins University, 733 North Broadway,*  
9 *Baltimore, MD 21205. <sup>4</sup>Shanghai Key Laboratory of Regulatory Biology, Institute of*  
10 *Biomedical Sciences, School of Life Sciences, East China Normal University, Shanghai,*  
11 *200241, China*

12

13

14

15

16

**MOL # 115303**

17 **Running title:** NPBA is a selective TASK-3 channel activator

18 **Corresponding Author:**

19 Zhaobing Gao, CAS Key Laboratory of Receptor Research, State Key Laboratory of Drug  
20 Research, Shanghai Institute of Materia Medica, Chinese Academy of Sciences, Shanghai,  
21 201203, China.

22 Email: zbgao@simm.ac.cn

23 Phone: 86-21-2023 9067

24 **Document statistics:**

25 Text pages: 30

26 Tables: 0

27 Figures: 6

28 References: 36

29 Abstract word count: 208

30 Introduction word count: 723

31 Discussion word count: 988

32

**MOL # 115303**

33 **Abstract**

34 The TASK-3 channel is a member of the K2P family that is important for the maintenance  
35 of the resting membrane potential. Previous studies have demonstrated that the TASK-3  
36 channel is involved in several physiological and pathological processes, including  
37 sleep/wake control, cognition and epilepsy. However, there is still a lack of selective  
38 pharmacological tools for TASK-3, which limits further research on channel function. In this  
39 work, using a high-throughput screen (HTS), we discovered that N-(2-((4-nitro-2-  
40 (trifluoromethyl)phenyl)amino)ethyl)benzamide (NPBA) showed excellent potency and  
41 selectivity as a novel TASK-3 activator. The molecular determinants of NPBA activation  
42 were then investigated by combining chimera and mutagenesis analysis. Two distant  
43 clusters of residues located at the extracellular end of the second transmembrane domain  
44 (TM2) (A105 and A108) and the intracellular end of the third transmembrane domain (TM3)  
45 (E157) were found to be critical for NPBA activation. We then compared the essentials of  
46 the actions of NPBA with inhalation anesthetics that nonselectively activate TASK-3 and  
47 found that they may activate TASK-3 channels through different mechanisms. Finally, the  
48 three residues A105, A108 and E157 were transplanted into the TASK-1 channel, which  
49 resists NPBA activation, and the constructed mutant TASK-1(G105A, V108A, A157E)  
50 showed dramatically increased activation by NPBA, which confirms the importance of  
51 these two distant clusters of residues.

**MOL # 115303**

## 52 **Introduction**

53 K2P channels conduct “leak” potassium currents, which play critical roles in the  
54 maintenance of the resting membrane potential. The K2P family currently has 15  
55 mammalian members, which can be divided into six distinct subfamilies based on structure  
56 and functional properties. The TWIK-related acid-sensitive K (TASK)-3 channel is a  
57 member of the K2P family and belongs to the TASK subfamily consisting of TASK-3, TASK-  
58 1, and TASK-5 (Enyedi and Czirjak, 2010). TASK-3 and TASK-1 are functional channels  
59 conducting currents highly sensitive to extracellular pH (Duprat et al., 1997; Kim et al.,  
60 2000; Rajan et al., 2000), while TASK-5 cannot be functionally expressed (Kim and  
61 Gnatenco, 2001).

62 Mainly expressed in the CNS, particularly in the cerebellum, hypothalamus and cortex  
63 (Talley et al., 2001), TASK-3 was proposed to be related to mood disorders, sleep/wake  
64 control and cognition (Gotter et al., 2011; Linden et al., 2007). The human TASK-3 mutation  
65 G236R has been identified as responsible for mental retardation associated with a rare  
66 maternally transmitted dysmorphism syndrome (Barel et al., 2008), and TASK-3 knock-out  
67 mice showed impaired working memory and altered circadian rhythms (Linden et al., 2007).  
68 Abundant TASK-3 expression was also found in the adrenal cortex, and it has been  
69 demonstrated that TASK-3 channel deletion in mice could recapitulate low-renin essential  
70 hypertension (Guagliardo et al., 2012). In addition, TASK-3 has been implicated in other  
71 disorders, including cancer (Mu et al., 2003), primary hyperaldosteronism (Davies et al.,  
72 2008), and epilepsy (Holter et al., 2005).

**MOL # 115303**

73 The TASK-3 channel, which is involved in multiple physiological and pathological  
74 processes, can be modulated by various endogenous neurochemicals, clinically active  
75 drugs, and physicochemical factors (Goldstein et al., 2001; Lesage, 2003; Talley et al.,  
76 2003). The TASK-3 channel is closed by extracellular acidification (Duprat et al., 1997; Kim  
77 et al., 2000; Rajan et al., 2000), and it is also inhibited by hormones and transmitters  
78 through GPCRs (Chemin et al., 2003; Mathie, 2007; Talley and Bayliss, 2002); this  
79 inhibition is now considered to be mediated by diacylglycerol (DAG) (Wilke et al., 2014).  
80 Moreover, the TASK-3 channel is an important target of inhalation anesthetics such as  
81 chloroform and respiratory stimulants such as doxapram (Cotten et al., 2006). In addition,  
82 the TASK-3 channel is sensitive to other small-molecule compounds, such as ruthenium  
83 red (Czirjak and Enyedi, 2002), anandamide (Berg et al., 2004), lidocaine (Kim et al., 2000)  
84 and bupivacaine (Meadows and Randall, 2001). However, all the small-molecule regulators  
85 above are nonselective, which limits their use as selective pharmacological tools for  
86 research on TASK-3. Currently, the only reported selective activator of TASK-3 is  
87 terbinafine, which has moderate potency with a maximum effect of ~ 2-fold and a pEC<sub>50</sub> of  
88 6.2 μM in the thallium flux assay, but the mechanism of action of this compound remains  
89 unknown (Wright et al., 2017).

90 In mechanistic research on TASK-3 activators, the mechanism of action of inhalation  
91 anesthetics on TASK-3 channels has been extensively studied and partially revealed.  
92 Specifically, M159, a residue located on the cytoplasmic side of TM3, was proposed to be  
93 the potential binding site of inhalation anesthetics (Andres-Enguix et al., 2007), and the

**MOL # 115303**

94 reliability of this conclusion was further evidenced by a later study using cysteine  
95 modification (Conway and Cotten, 2012). In addition, amino acids 243 to 248 (VLRFLT),  
96 located in the junction of TM4 and the carboxyl terminus (Ct), were also identified as  
97 essential for activation by inhalation anesthetics (Patel et al., 1999), and this region was  
98 also demonstrated to be important for the regulation of GPCR or other intracellular factors  
99 (Talley and Bayliss, 2002). Several studies on TREK-1 (K<sub>2P</sub>2.1) concluded that the TM4–  
100 Ct junction was critical for the conduction of conformational transmission from the Ct to the  
101 pore of the channel, which could be disturbed by a triple glycine mutation K<sub>2P</sub>2.1-3G  
102 (Bagriantsev et al., 2012; Bagriantsev et al., 2011). The up and down states of TM4 have  
103 been proven to represent different conductive states that involve the conformational  
104 transmission (Dong et al., 2015).

105 In this study, we searched for better small-molecule activators of TASK-3 by high-  
106 throughput screening (HTS) and identified NPBA as a novel selective agonist of the TASK-  
107 3 channel. Furthermore, by adopting various mutagenesis analyses, we found three  
108 residues, A108, A105 and E157 that were important for NPBA activation. In addition, we  
109 found that the selective activator we identified shared some common key residues with  
110 inhalation anesthetics but may conduct channel activation through a different mechanism.

## 111 **Materials and Methods**

### 112 **Plasmid construction**

113 Human TASK-3, human TASK-1, and human TRESK were gifts from Dr Min Li (Johns

**MOL # 115303**

114 Hopkins University, USA). EGFP, human TREK-1 and rat THIK1 were provided by Jia Li  
115 (Shanghai Institute of Materia Medica, China), Yang Li (Shanghai Institute of Materia  
116 Medica, China) and Haijun Chen (State University of New York, USA). Point mutations of  
117 TASK channels were introduced using the QuikChange II Site-directed Mutagenesis Kit  
118 (Stratagene), and chimeras of the TASK channel were constructed using the In-Fusion HD  
119 Cloning Kit (TaKaRa). All constructs were verified by sequencing.

120 **Cell culture and transient transfection**

121 CHO-K1 cells were cultured in DMEM/F12 (Gibco) with 10% FBS (Gibco). Twenty-four  
122 hours prior to transfection, the cells were split into 6-well dishes. Plasmids encoding the  
123 EGFP and K2P channels were cotransfected with Lipofectamine 3000 reagent (Invitrogen)  
124 according to the manufacturer's instructions.

125 **Electrophysiological recording**

126 To measure the currents of the K2P channels expressed in CHO-K1 cells, standard whole-  
127 cell patch clamping experiments were performed at room temperature. Pipettes with  
128 resistance ranging from 2.0 to 5.0 M $\Omega$  were pulled using borosilicate glass capillaries  
129 (World Precision Instruments). During the recording process, constant perfusion of bath  
130 solution was maintained using a BPS perfusion system (ALA Scientific). The pipette  
131 solution contained the following: 145 mM KCl, 1 mM MgCl<sub>2</sub>, 5 mM EGTA, and 10 mM  
132 HEPES (pH 7.3 with KOH). The bath solution contained the following: 140 mM NaCl, 5 mM  
133 KCl, 2 mM CaCl<sub>2</sub>, 1 mM MgCl<sub>2</sub>, 10 mM glucose and 10 mM HEPES (pH 7.4 with NaOH).

**MOL # 115303**

134 The whole-cell currents were recorded using an EPC-10 amplifier (HEKA), and signals  
135 were filtered at 2 kHz, digitized using a DigiData 1440A, and analyzed with pClamp 9.2  
136 software (Molecular Devices). The series resistance was compensated by 60%.

137 **Homology Modeling**

138 The structures of the TASK-3 channel were constructed based on the crystal structures of  
139 the TREK-2 channel (PDB code 4BW5 and 4XDJ, identity: 31%) by using Modeler (Sali  
140 and Blundell, 1993), which are reported as the conductive and nonconductive states,  
141 separately. Multiple sequence alignment was generated by using the Clustal Omega web  
142 server (<https://www.ebi.ac.uk/Tools/msa/clustalo>).

143 **Statistics**

144 Patch-clamp data were processed using Clampfit 10.2 (Molecular Devices) and then  
145 analyzed in GraphPad Prism 5 (GraphPad Software). Dose–response curves were fitted  
146 with the Hill equation,  $E = E_{max}/[1 - (EC_{50}/C)^P]$ , where EC<sub>50</sub> is the drug concentration  
147 producing the half-maximum response. The data are shown as the means ± SEM, and the  
148 significance was estimated using one-way ANOVA followed by Dunnett's post hoc test.  
149 Statistical significance: \* P < 0.05, \*\* P < 0.01, \*\*\* P < 0.001.



**MOL # 115303**

## 150 **Results**

### 151 **Identification of NPBA as a selective TASK-3 activator**

152 To address the lack of selective pharmacology tools for the TASK-3 channel, we developed  
153 an HTS to discover selective small-molecule TASK-3 modulators. Before the HTS, HEK293  
154 cell lines stably expressing human TASK-3 or its closest homologue TASK-1 were  
155 established because selective active compounds for the TASK subfamily were more likely  
156 to exhibit selectivity among the  $K_{2P}$  family. Then, the channel activity was measured by a  
157 thallium flux assay as in the previous work (Yu et al., 2015; Yue et al., 2016).

158 Within the project, more than 300,000 compounds were screened, of which 1417  
159 compounds were identified as TASK-3 activators. Among these active compounds, N-(2-  
160 ((4-nitro-2-(trifluoromethyl)phenyl)amino)ethyl)benzamide (NPBA) exhibited the best  
161 potency for TASK-3 activation and showed good selectivity between TASK channels. Fig.  
162 1A shows the molecular structure of NPBA.

163 To confirm the activation of NPBA and to estimate its potency, whole-cell patch clamp  
164 recordings were performed. CHO-K1 cells transiently transfected with wild-type human  
165 TASK-3 or other  $K_{2P}$  channels were used for the recording, and we ran a voltage-ramp  
166 protocol from -130 mV to 20 mV to obtain the I-V curve. The current at 0 mV was chosen  
167 to measure the potency of NPBA toward different channels. For the dose-response curve  
168 study, we tested concentrations of NPBA ranging from 0.1  $\mu$ M to 30  $\mu$ M, as the compound

**MOL # 115303**

169 cannot be completely dissolved at a higher concentration of 100  $\mu$ M. NPBA showed  
170 reversible dose-dependent activation of TASK-3 whole-cell currents with an  $EC_{50}$  of 6.7  $\mu$ M,  
171 and the currents were increased by up to ~6-fold at a concentration of 10  $\mu$ M (Fig. 1, B  
172 and C). We also investigated the effects of 10  $\mu$ M NPBA on other  $K_{2PS}$ , including TASK-1,  
173 TREK-1, TRESK and THIK-1, but no activation was detected in these channels (Fig. 1D),  
174 suggesting excellent selectivity of NPBA towards TASK-3 channels. As the closest  
175 homologue of TASK-3, TASK-1 was also tested in a dose-response curve study, and it was  
176 reversibly inhibited by NPBA in a dose-dependent manner, with an  $IC_{50}$  of 7.5  $\mu$ M (Fig. 1,  
177 E and F). These results indicated that NPBA was a potent activator of the TASK-3 channel  
178 and has good selectivity.

179 **The A108 residue located at the extracellular end of TM2 is crucial for**  
180 **activation by NPBA**

181 To identify regions of the TASK-3 channel that are necessary for activation by NPBA,  
182 TASK-3 and TASK-1 subunits were used to make chimeric constructs because they shared  
183 highly homologous sequences but showed greatly different responses to NPBA.

184 Using In-Fusion cloning technology, we first replaced the N-terminus of TASK-3 with a  
185 homologous sequence from TASK-1 and gradually extended the replaced region. We  
186 constructed T1-85-T3, in which amino acids 1-85 of TASK-3 were replaced by the  
187 corresponding part of TASK-1, and we constructed T1-131-T3, T1-169-T3 and T1-209-T3  
188 in the same manner. Then, the effects of NPBA on these chimeras were tested at a

**MOL # 115303**

189 concentration of 10  $\mu$ M. The first chimera, T1-85-T3, with the junction in the first pore  
190 domain, retained the activation by NPBA (Fig. 2A), while the other chimeras with the  
191 junction at or after position 131 in this series were not activated by NPBA (Fig. 2, B-D).  
192 These results indicated that there were key NPBA determinants within amino acids 85-131.

193 A mutagenesis scan was then performed to investigate the critical residues in this region.  
194 We tested the effects of swapping each of the amino acids that differed between TASK-3  
195 and TASK-1 within section 85-131 (Fig. 2E). In the TASK-3 channel, these four amino acids  
196 were individually replaced by those in the homologous sites of TASK-1. Among the four  
197 TASK-3 mutations (Fig. 2E), A105G moderately impaired the activation by NPBA, and the  
198 current was increased by  $\sim$ 3-fold under 10  $\mu$ M NPBA (Figs. 2F and 4G), while A108V  
199 completely abrogated the activation by NPBA and showed inhibition at 10  $\mu$ M NPBA (Figs.  
200 2G and 4G). However, the other two mutants, G102S and V115L showed an NPBA  
201 phenotype that was indistinguishable from the wild type (Fig. 4G).

202 Since the alanine at position 108 (A108) seemed to be crucial for activation by NPBA, we  
203 replaced this alanine with various other amino acids, including phenylalanine, leucine,  
204 isoleucine, glycine, tyrosine, cysteine, and serine. Among all these A108 mutants, only  
205 A108G or A108S showed current activation in response to by 10  $\mu$ M NPBA, while all other  
206 mutant showed the same current inhibition as A108V (Fig. 3A). Furthermore, we performed  
207 alanine scanning mutagenesis within the residues around A108 and evaluated the  
208 responses under 10  $\mu$ M NPBA. Among the nine mutant channels, four mutations (T103A,  
209 D104A, F109A, and M111A) eliminated activation by NPBA and showed current inhibition

**MOL # 115303**

210 by NPBA, while mutations of the remaining five residues (P101A, G102A, G106A, K107A,  
211 and C110A) showed only a slight decrease in the activation degree resulting from NPBA  
212 (Fig. 3B). Taken together, these findings suggested that the residues around A108 played  
213 a crucial role in NPBA activation on the TASK-3 channel.

214 **A TASK-1 mutant with alanine at position 108 resists NPBA activation**

215 Since the TASK-3 mutant A108V showed a total loss of NPBA activation, we wondered  
216 whether the corresponding TASK-1 mutant V108A would gain activation by NPBA. As  
217 shown in Fig. 3C, however, TASK-1(V108A) could not be activated by 10  $\mu$ M NPBA. A  
218 double-mutant TASK-1 channel (G105A, V108A) was then constructed by introducing  
219 G105A into TASK-1(V108A). We found that the newly constructed mutant channel was  
220 also unable to be activated by NPBA (Fig. 3D). In contrast, it showed an inhibition similar  
221 to that in the wild-type TASK-1 or TASK-1(V108A). These results implied that these  
222 residues on TM2 were not the only determinants responsible for the different NPBA  
223 phenotypes of TASK-1 and TASK-3.

224 **The intracellular end of TM3 is important for NPBA activation**

225 Based on the results above, we concluded that there should be other important residues  
226 for NPBA activation in addition to A105 and A108. To identify these unknown determinants,  
227 we constructed another series of chimeras. In this group of chimeras, the C-terminal of  
228 TASK-3 was replaced by the homologous sequence of TASK-1, and the junction was

**MOL # 115303**

229 moved forward gradually. We constructed T3-240-T1 as the protein sequence after position  
230 240 of TASK-3 was replaced by the corresponding section of TASK-1 and constructed T3-  
231 209-T1, T3-169-T1 and T3-131-T1 in the same manner. We then tested the effects of  
232 NPBA at a concentration of 10  $\mu$ M. With the junction moving forward, T3-240-T1, T3-209-  
233 T1, and T3-169-T1 could all be activated by NPBA (Fig. 4, A-C), while the last chimera T3-  
234 131-T1 could not be activated significantly by 10  $\mu$ M NPBA (Fig. 4D). These results  
235 suggested that there were determinants for NPBA activation within section 131-169 in  
236 addition to 85-131.

237 Next, we performed scanning mutagenesis within amino acids 131-169 of TASK-3, and 16  
238 mutants were constructed and evaluated (Fig. 4, E and G). Among these mutations, the  
239 mutation E157A weakened NPBA activation the most, and the mutant currents showed  
240 only a 2-fold enhancement under 10  $\mu$ M NPBA (Fig. 4F). There are also other mutations  
241 that impaired the activation, such as M168I and K141H, which showed a moderate  $\sim$ 3-fold  
242 current activation in response to 10  $\mu$ M NPBA (Fig. 4G).

243 Since the glutamic acid at position 157 (E157) seems to be important for NPBA activation,  
244 we further changed this negatively charged amino acid to negatively charged aspartic acid,  
245 positively charged arginine or neutral glutamine and determined the effects of 10  $\mu$ M NPBA  
246 on these mutants. Both E157D and E157R showed the same NPBA phenotype as E157A,  
247 with only a 2-fold current enhancement under 10  $\mu$ M NPBA. However, the E157Q current  
248 was activated by 10  $\mu$ M NPBA as effectively the wild-type TASK-3 channel, showing 6-fold  
249 activation under 10  $\mu$ M NPBA (Fig. 5A). These results suggested that E157 is also an

**MOL # 115303**

250 important residue for NPBA activation, and the volume rather than the charge of the residue  
251 at position 157 is the key characteristic necessary to achieve a potent activation by NPBA.

252 **NPBA activates TASK-3 through a different mechanism from inhalation**  
253 **anesthetics**

254 E157 was predicted to be located in the intracellular end of TM3 on the basis of hydrophobic  
255 analysis (Kim et al., 2000) and is very close to M159 (Figs. 4E and 6G), a residue reported  
256 to be the binding site of nonselective inhalation anesthetics. Thus, we wondered whether  
257 activation by NPBA and activation by inhalation anesthetics occurred through a common  
258 mechanism. In this study, chloroform was selected as a representative inhalation  
259 anesthetic and increased the wild-type TASK-3 current approximately 2-fold at a  
260 concentration of 5 mM (Fig. 5, B and J), which is consistent with previous results (Andres-  
261 Enguix et al., 2007). Thereafter, we determined and compared the effects of NPBA and  
262 chloroform on the mutant channels that have been reported to show impaired anesthetic  
263 activation. First, we constructed the mutant that showed increased basal currents and  
264 resistance to activation by inhalation anesthetics (Conway and Cotten, 2012). M159W  
265 completely abrogated the activation by 5 mM chloroform, while activation by NPBA was  
266 partially retained (Fig. 5, C, D and J). Then, we constructed the mutant R245W with a large  
267 tryptophan predicted to occupy the space around M159, similar to M159W (Fig. 6G).  
268 Notably, this alteration abolished activation by both NPBA and chloroform and showed a  
269 different NPBA phenotype from that of M159W (Fig. 5 E, F and J). In addition, we  
270 constructed a TASK-3 mutant 242-3G with three residues, V242-V243-L244, replaced by

**MOL # 115303**

271 glycines, based on a  $K_{2P}2.1$ -3G mutant predicted to uncouple the cross-talk between the  
272 pore and carboxyl terminus (Bagriantsev et al., 2012). Subsequently, 5 mM chloroform  
273 failed to induce an increase in current in the 242-3G mutant and instead showed an  
274 inhibitory effect on the current (Fig. 5, H and J), suggesting that this triple glycine mutation  
275 also affects the TASK-3 channel. However, the activation by NPBA was retained in the 242-  
276 3G mutant, with a potency of 2-fold under a concentration of 10 mM (Fig. 5, G and J).  
277 Finally, we tested the effect of 5 mM chloroform on the A108V mutant that completely  
278 abolished NPBA activation (Fig. 2G). The activation degree of 5 mM chloroform for A108V  
279 was indistinguishable from that for the wild-type TASK-3 channel (Fig. 5, I and J). Taken  
280 together, these results demonstrated that though activation by NPBA and inhalation  
281 anesthetics shared some key residues, such as M159, they were likely to activate the  
282 channel through different action mechanisms.

283 **A TASK-1 mutant with three key residues swapped gains NPBA activation**

284 Since the amino acids 131-169 were also shown to be vital regions for NPBA activation  
285 and E157 seemed to be the most important residue in this region, we transplanted E157  
286 into the mutant channel TASK-1(G105A,V108A) to construct the mutant TASK-1(G105A,  
287 V108A, A157E), and then we determined the effect of 10  $\mu$ M NPBA on this triple-mutant  
288 channel. The logic here was to try to construct a TASK-1 mutant that could be activated by  
289 NPBA to confirm the importance of these residues. Dramatically, TASK-1(G105A, V108A,  
290 A157E) gained NPBA activation, and the current in the mutant showed a 1.5-fold increase  
291 under a NPBA concentration of 10  $\mu$  M (Fig. 6, A and C). In contrast, a mutant with two

**MOL # 115303**

292 sites changed, TASK-1(V108A, A157E) did not gain activation by 10  $\mu$  M NPBA (Fig. 6, B  
293 and C). Notably, TASK-1(G105A, V108A, A157E) showed an NPBA phenotype combining  
294 the responses of TASK-1 and TASK-3. After the administration of NPBA, the mutant  
295 currents decreased initially for seconds and then increased gradually, displaying an inward  
296 hook on the time course plot (Fig. 6A). We speculated that the intrinsic inhibition of TASK-  
297 1 perhaps counteracts the acquired potentiation from the three mutations (G105A, V108A,  
298 A157E), resulting in a weaker activation of the current amplitude than that of the wild-type  
299 TASK-3 channel. These results demonstrated that A108, A105 and E157 were important  
300 for activation (Fig. 6D).

301 Based on the crystal structures of TREK-2, we created an open-state homology model of  
302 TASK-3 (Fig. 6E). Structurally, the key residues A105 and A108 lie at the extracellular end  
303 of TM2, a pore-lining helix adjacent to P1 and P2 (Fig. 6, D-F), while the third key residue  
304 E157 is located in the intracellular end of TM3 (Fig. 6, D, E and G). Notably, these two  
305 regions are separated by a long distance of approximately 26.6 Å (Fig. 6E).

306 **Discussion**

307 Among K2P channels, the TASK-3 channel has been implicated in a number of normal  
308 physiological processes or disorders, but few selective TASK-3 channel modulators have  
309 been identified, which hinders the understanding of channel function in physiology.  
310 Terbinafine, an antifungal medication, was the first and previously the only selective  
311 activator of TASK-3 reported, but this compound only has a moderate activation effect. In



**MOL # 115303**

312 the present work, we identified NPBA as a novel agonist of the TASK-3 channel by HTS.  
313 NPBA produces ~6-fold activation under a concentration of 10  $\mu$ M (Fig. 1B) and is thus  
314 more potent than terbinafine, though the EC<sub>50</sub> of NPBA (6.7  $\mu$ M) is almost equal to that  
315 of terbinafine (6.2  $\mu$ M) (Fig. 1C). In addition, NPBA also has good selectivity (Fig. 1C),  
316 which makes it a useful pharmacological probe for in vitro studies of TASK-3 function and  
317 in further studies intended for therapeutic intervention.

318 The study of the molecular mechanisms of modulators is an important aspect of ion  
319 channel research. For TASK-3, previous studies mainly focused on the regulation of pH  
320 and inhalation anesthetics. Though some explicit results have been obtained (Andres-  
321 Enguix et al., 2007; Conway and Cotten, 2012), fewer novel elements in the activation  
322 mechanism of TASK-3 have been reported in recent years, which may be due to the lack  
323 of novel modulators of TASK-3. Adopting the classical chimera strategy and various  
324 mutagenesis analyses in this work, we found several residues that are important for NPBA  
325 activation, whose alteration could significantly impair NPBA activation (Figs. 2, 3 and 4).  
326 By transplanting three of these residues, A105, A108 and E157, into the TASK-1 channel,  
327 which resists activation by NPBA, the TASK-1 mutant TASK-1 (G105A, V108A, A157E)  
328 was constructed and dramatically gained activation by NPBA (Fig. 6, A and C). This gain  
329 of activation is more convincing because no binding assay or cocrystallization research  
330 has been performed in previous studies of TASK-3, which further confirms the importance  
331 of these residues. Among the three residues, A108 and A105 lie at the proximal  
332 amphipathic end of TM2 adjacent to P1 and P2 (Fig. 6, D and F), which may be related to

**MOL # 115303**

333 selective filter gating, while E157 is spatially adjacent to the distal end of TM4, the up and  
334 down states of which have been proven to represent different conductive states (Fig.  
335 6G)(Dong et al., 2015). These residues have never been mentioned in previous studies of  
336 TASK-3 and may provide clues for the understanding of the gate mechanism of TASK-3.

337 The mechanism of the activation of TASK-3 by inhalation anesthetics has been partially  
338 revealed. The binding site of these molecules was believed to be located on the  
339 intracellular side of TM3 near M159 (Andres-Enguix et al., 2007; Conway and Cotten,  
340 2012). In addition, the amino acids 243-248 were also involved in the inhalation anesthetic  
341 activation (Talley and Bayliss, 2002). In the present work, by comparing the phenotypes of  
342 the response to NPBA and chloroform in multiple TASK-3 mutants, we found that some  
343 mutants, such as R245W, affected activations by both NPBA and chloroform (Fig. 5 E and  
344 F). However, the elements that are vital for the activation of NPBA and chloroform did not  
345 overlap perfectly. Specifically, the most crucial mutant for NPBA activation, A108V, did not  
346 change the chloroform activation (Figs. 2G and 5I); the mutant 242-3G retained NPBA  
347 activation, although chloroform activation was abolished (Fig. 5, G and H). Among the  
348 mutations that weakened the activation by chloroform, M159W is a classic mutation that  
349 has proven to be effective by occupying the space around the binding site of chloroform  
350 with a tryptophan and mimicking a chloroform-bound more conductive conformation.  
351 Interestingly, R245W seems to affect the activation of chloroform in a similar manner since  
352 R245 is spatially near M159. However, NPBA activation was partially retained in M159W,  
353 suggesting that NPBA does not share M159 as a binding site with chloroform. Accordingly,

**MOL # 115303**

354 the activation effect of NPBA on wild-type TASK3 was tested in the presence of 10 mM  
355 chloroform, a saturated concentration of the inhalation anesthetic. We found that NPBA  
356 further significantly potentiated the increased currents by chloroform (Supplementary Fig.  
357 2). These results suggest that the novel activator NPBA may activate TASK-3 differently  
358 from inhalation anesthetics.

359 The TM4 and Ct domains in K2Ps have proven to be important regions for a range of  
360 signaling inputs within the cell, including temperature (Maingret et al., 2000), mechanical  
361 force (Patel et al., 1998), and phosphorylation (Bagriantsev et al., 2012). Notably, the  
362 crosstalk between the two regions can be broken by the 242-3G mutation (Bagriantsev et  
363 al., 2012). In our work, the 242-3G mutation completely abolished the activation by  
364 chloroform, which could be explained by the fact that activation by chloroform depends on  
365 the relay from the Ct domain to TM4 or that this 3G mutation causes conformational  
366 changes in the anesthetic pocket. However, NPBA activation was retained in 242-3G,  
367 indicating that the binding site of NPBA is upstream of the link between TM4 and the Ct  
368 domain. Finally, A108, a brand new residue we identified, was found to be necessary only  
369 for activation by NPBA rather than chloroform. Because mutating 3 residues (G105A,  
370 V108A, and A157E) in TASK-1 partially conferred NPBA activation on TASK-1, we  
371 speculated that a long-range coupling between the extracellular segment around A108 and  
372 the intracellular domains around E157 might be involved in NPBA-induced activation. To  
373 elucidate the specific mechanism underlying potential cooperation, further studies, such as  
374 binding assays, computational simulations and crystallization research, are necessary.

**MOL # 115303**

375 In conclusion, we have described the ability of a novel compound, NPBA, to activate the  
376 TASK-3 channel. This compound also displays marked specificity within the K<sub>2</sub>P group  
377 and may therefore be a good pharmacological tool for TASK-3 research. Several additional  
378 elements that are important for NPBA action have also been uncovered in our work. This  
379 finding provides a strategy to identify more novel TASK-3 activators, and the key residues  
380 we found, such as A108, may promote research on the gate mechanism of K<sub>2</sub>P channels.

381

382 **Author Contributions**

383 Research design: Gao

384 Conducted experiments: Tian, Lan,

385 Performed data analysis: Tian, Lan, Qiu, Li and Yang

386 Wrote the manuscript: Tian, Gao

387 **References**

388 Andres-Enguix I, Caley A, Yustos R, Schumacher MA, Spanu PD, Dickinson R, Maze M and Franks NP  
389 (2007) Determinants of the anesthetic sensitivity of two-pore domain acid-sensitive  
390 potassium channels: molecular cloning of an anesthetic-activated potassium channel from  
391 *Lymnaea stagnalis*. *The Journal of biological chemistry* **282**:20977-20990.

392 Bagriantsev SN, Clark KA and Minor DL, Jr. (2012) Metabolic and thermal stimuli control K(2P)2.1  
393 (TREK-1) through modular sensory and gating domains. *The EMBO journal* **31**:3297-3308.

394 Bagriantsev SN, Peyronnet R, Clark KA, Honore E and Minor DL, Jr. (2011) Multiple modalities converge  
395 on a common gate to control K<sub>2</sub>P channel function. *The EMBO journal* **30**:3594-3606.

396 Barel O, Shalev SA, Ofir R, Cohen A, Zlotogora J, Shorer Z, Mazor G, Finer G, Khateeb S, Zilberberg N  
397 and Birk OS (2008) Maternally inherited Birk Barel mental retardation dysmorphism

**MOL # 115303**

- 398 syndrome caused by a mutation in the genomically imprinted potassium channel KCNK9.  
399 *American journal of human genetics* **83**:193-199.
- 400 Berg AP, Talley EM, Manger JP and Bayliss DA (2004) Motoneurons express heteromeric TWIK-related  
401 acid-sensitive K<sup>+</sup> (TASK) channels containing TASK-1 (KCNK3) and TASK-3 (KCNK9) subunits.  
402 *The Journal of neuroscience : the official journal of the Society for Neuroscience* **24**:6693-  
403 6702.
- 404 Chemin J, Girard C, Duprat F, Lesage F, Romey G and Lazdunski M (2003) Mechanisms underlying  
405 excitatory effects of group I metabotropic glutamate receptors via inhibition of 2P domain K<sup>+</sup>  
406 channels. *The EMBO journal* **22**:5403-5411.
- 407 Conway KE and Cotten JF (2012) Covalent modification of a volatile anesthetic regulatory site activates  
408 TASK-3 (KCNK9) tandem-pore potassium channels. *Molecular pharmacology* **81**:393-400.
- 409 Cotten JF, Keshavaprasad B, Laster MJ, Eger EI, 2nd and Yost CS (2006) The ventilatory stimulant  
410 doxapram inhibits TASK tandem pore (K2P) potassium channel function but does not affect  
411 minimum alveolar anesthetic concentration. *Anesthesia and analgesia* **102**:779-785.
- 412 Czirjak G and Enyedi P (2002) Formation of functional heterodimers between the TASK-1 and TASK-3  
413 two-pore domain potassium channel subunits. *The Journal of biological chemistry* **277**:5426-  
414 5432.
- 415 Davies LA, Hu C, Guagliardo NA, Sen N, Chen X, Talley EM, Carey RM, Bayliss DA and Barrett PQ (2008)  
416 TASK channel deletion in mice causes primary hyperaldosteronism. *Proceedings of the*  
417 *National Academy of Sciences of the United States of America* **105**:2203-2208.
- 418 Dong YY, Pike AC, Mackenzie A, McClenaghan C, Aryal P, Dong L, Quigley A, Grieben M, Goubin S,  
419 Mukhopadhyay S, Ruda GF, Clausen MV, Cao L, Brennan PE, Burgess-Brown NA, Sansom MS,  
420 Tucker SJ and Carpenter EP (2015) K2P channel gating mechanisms revealed by structures of  
421 TREK-2 and a complex with Prozac. *Science* **347**:1256-1259.
- 422 Duprat F, Lesage F, Fink M, Reyes R, Heurteaux C and Lazdunski M (1997) TASK, a human background  
423 K<sup>+</sup> channel to sense external pH variations near physiological pH. *The EMBO journal* **16**:5464-  
424 5471.
- 425 Enyedi P and Czirjak G (2010) Molecular background of leak K<sup>+</sup> currents: two-pore domain potassium  
426 channels. *Physiological reviews* **90**:559-605.
- 427 Goldstein SA, Bockenhauer D, O'Kelly I and Zilberberg N (2001) Potassium leak channels and the KCNK  
428 family of two-P-domain subunits. *Nature reviews Neuroscience* **2**:175-184.
- 429 Gotter AL, Santarelli VP, Doran SM, Tannenbaum PL, Kraus RL, Rosahl TW, Meziane H, Montial M, Reiss  
430 DR, Wessner K, McCampbell A, Stevens J, Brunner JI, Fox SV, Uebele VN, Bayliss DA, Winrow  
431 CJ and Renger JJ (2011) TASK-3 as a potential antidepressant target. *Brain research* **1416**:69-  
432 79.
- 433 Guagliardo NA, Yao J, Hu C, Schertz EM, Tyson DA, Carey RM, Bayliss DA and Barrett PQ (2012) TASK-3  
434 channel deletion in mice recapitulates low-renin essential hypertension. *Hypertension*  
435 **59**:999-1005.
- 436 Holter J, Carter D, Leresche N, Crunelli V and Vincent P (2005) A TASK3 channel (KCNK9) mutation in a  
437 genetic model of absence epilepsy. *Journal of molecular neuroscience : MN* **25**:37-51.
- 438 Kim D and Gnatenco C (2001) TASK-5, a new member of the tandem-pore K(+) channel family.  
439 *Biochemical and biophysical research communications* **284**:923-930.
- 440 Kim Y, Bang H and Kim D (2000) TASK-3, a new member of the tandem pore K(+) channel family. *The*  
441 *Journal of biological chemistry* **275**:9340-9347.

**MOL # 115303**

- 442 Lesage F (2003) Pharmacology of neuronal background potassium channels. *Neuropharmacology*  
443 **44**:1-7.
- 444 Linden AM, Sandu C, Aller MI, Vekovischeva OY, Rosenberg PH, Wisden W and Korpi ER (2007) TASK-3  
445 knockout mice exhibit exaggerated nocturnal activity, impairments in cognitive functions, and  
446 reduced sensitivity to inhalation anesthetics. *The Journal of pharmacology and experimental*  
447 *therapeutics* **323**:924-934.
- 448 Maingret F, Lauritzen I, Patel AJ, Heurteaux C, Reyes R, Lesage F, Lazdunski M and Honore E (2000)  
449 TREK-1 is a heat-activated background K(+) channel. *The EMBO journal* **19**:2483-2491.
- 450 Mathie A (2007) Neuronal two-pore-domain potassium channels and their regulation by G protein-  
451 coupled receptors. *The Journal of physiology* **578**:377-385.
- 452 Meadows HJ and Randall AD (2001) Functional characterisation of human TASK-3, an acid-sensitive  
453 two-pore domain potassium channel. *Neuropharmacology* **40**:551-559.
- 454 Mu D, Chen L, Zhang X, See LH, Koch CM, Yen C, Tong JJ, Spiegel L, Nguyen KC, Servoss A, Peng Y, Pei L,  
455 Marks JR, Lowe S, Hoey T, Jan LY, McCombie WR, Wigler MH and Powers S (2003) Genomic  
456 amplification and oncogenic properties of the KCNK9 potassium channel gene. *Cancer cell*  
457 **3**:297-302.
- 458 Patel AJ, Honore E, Lesage F, Fink M, Romey G and Lazdunski M (1999) Inhalational anesthetics  
459 activate two-pore-domain background K+ channels. *Nature neuroscience* **2**:422-426.
- 460 Patel AJ, Honore E, Maingret F, Lesage F, Fink M, Duprat F and Lazdunski M (1998) A mammalian two  
461 pore domain mechano-gated S-like K+ channel. *The EMBO journal* **17**:4283-4290.
- 462 Rajan S, Wischmeyer E, Xin Liu G, Preisig-Muller R, Daut J, Karschin A and Derst C (2000) TASK-3, a  
463 novel tandem pore domain acid-sensitive K+ channel. An extracellular histidine as pH sensor.  
464 *The Journal of biological chemistry* **275**:16650-16657.
- 465 Sali A and Blundell TL (1993) Comparative protein modelling by satisfaction of spatial restraints.  
466 *Journal of molecular biology* **234**:779-815.
- 467 Talley EM and Bayliss DA (2002) Modulation of TASK-1 (Kcnk3) and TASK-3 (Kcnk9) potassium  
468 channels: volatile anesthetics and neurotransmitters share a molecular site of action. *The*  
469 *Journal of biological chemistry* **277**:17733-17742.
- 470 Talley EM, Sirois JE, Lei Q and Bayliss DA (2003) Two-pore-Domain (KCNK) potassium channels:  
471 dynamic roles in neuronal function. *The Neuroscientist : a review journal bringing*  
472 *neurobiology, neurology and psychiatry* **9**:46-56.
- 473 Talley EM, Solorzano G, Lei Q, Kim D and Bayliss DA (2001) Cns distribution of members of the two-  
474 pore-domain (KCNK) potassium channel family. *The Journal of neuroscience : the official*  
475 *journal of the Society for Neuroscience* **21**:7491-7505.
- 476 Wilke BU, Lindner M, Greifenberg L, Albus A, Kronimus Y, Bunemann M, Leitner MG and Oliver D  
477 (2014) Diacylglycerol mediates regulation of TASK potassium channels by Gq-coupled  
478 receptors. *Nature communications* **5**:5540.
- 479 Wright PD, Veale EL, McCoull D, Tickle DC, Large JM, Ococks E, Gothard G, Kettleborough C, Mathie A  
480 and Jerman J (2017) Terbinafine is a novel and selective activator of the two-pore domain  
481 potassium channel TASK3. *Biochemical and biophysical research communications* **493**:444-  
482 450.
- 483 Yu H, Zou B, Wang X and Li M (2015) Effect of tyrphostin AG879 on Kv 4.2 and Kv 4.3 potassium  
484 channels. *British journal of pharmacology* **172**:3370-3382.
- 485 Yue JF, Qiao GH, Liu N, Nan FJ and Gao ZB (2016) Novel KCNQ2 channel activators discovered using

**MOL # 115303**

486 fluorescence-based and automated patch-clamp-based high-throughput screening  
487 techniques. *Acta pharmacologica Sinica* **37**:105-110.

488 **Footnotes**

489 This work was supported by the National Science Fund of Distinguished Young Scholars  
490 (81825021), the National Natural Science Foundation of China (81773707), and the  
491 Strategic Leading Science and Technology Projects of Chinese Academy of Sciences  
492 (XDA12040211, XDA12050308).

493 **Figure Legends**

494 **Figure 1. NPBA selectively activates TASK-3 channel in a dose-depend**  
495 **manner.**

496 **(A)** Chemical structure of NPBA.

497 **(B)** Typical whole-cell current traces recorded from CHO-K1 cells overexpressing the  
498 TASK-3 channel with normal bath solution or that with 10  $\mu$ M NPBA. Currents at 0 mV  
499 was plotted over time to reveal changes in response to NPBA. Period with NPBA  
500 administration is marked by an orange bar and circle filled with orange, while circles  
501 filled with blue shown currents with normal bath solution administration. Another  
502 version of typical traces and timecourse with complete washout phase was shown in  
503 Supplementary Fig 1.

**MOL # 115303**

504 **(C)** Dose-dependent curve of NPBA on TASK-3 channel. Each point represents the mean  
505 with bars of S.E.M (n > 6).

506 **(D)** The statistics of the activation of 10  $\mu$ M or 30  $\mu$ M NPBA for TASK-3, TASK-1, TREK-1,  
507 TRESK, and THIK-1 channels showing differences in NPBA sensitivity, with effects of  
508 10  $\mu$ M shown in orange while effects of 30  $\mu$ M shown in red.

509 **(E)** Typical whole-cell current traces recorded from CHO-K1 cells overexpressing the  
510 TASK-1 channel with normal bath solution or that with 10  $\mu$ M NPBA.

511 **(F)** Dose-dependent curve of NPBA on TASK-1 channel. Each point represents the mean  
512 with bars of S.E.M (n > 4).

513 **Figure 2. Segment 85-131 is important for TASK-3 activation.**

514 **(A-D)** Typical whole-cell current traces and time courses recorded from CHO-K1 cells  
515 overexpressing the T1-85-T3 **(A)**, T1-131-T3 **(B)**, T1-169-T3 **(C)**, or T1-240-T3 **(D)** mutant  
516 channel with 10  $\mu$ M NPBA. Protein secondary structure of chimera is shown beside the  
517 current traces, and section of TASK-3 appears in orange while section of TASK-1 appears  
518 in blue.

519 **(E)** Sequence alignment of TASK-3 and TASK-1 for the residues 85-131. Residues different  
520 in TASK channels appear in jacinth. The pore domain and TM2 are marked above the  
521 sequences. Residues revealed important in swapping mutagenesis are marked with



**MOL # 115303**

522 arrows.

523 **(F and G)** Typical whole-cell current traces and time courses recorded from CHO-K1 cells  
524 overexpressing the TASK-3(A105G) **(F)** or TASK-3(A108V) **(G)** mutant with 10  $\mu$ M NPBA.

525 **Figure 3. Residues around A108 is important for NPBA activation.**

526 **(A)** The statistics of the activation of 10 $\mu$ M NPBA for wild-type TASK-3 (n=10), A108G  
527 (n=4), A108S (n=4), A108C (n=4), A108V (n=7), A108L (n=4), A108I (n=4), A108F  
528 (n=4), and A108Y (n=4).

529 **(B)** The statistics of the activation of 10 $\mu$ M NPBA for wild-type TASK-3 (n=10), P101A (n=4),  
530 T103A (n=5), D104A (n=5), G106A (n=4), K107A (n=6), F109A (n=4), C110A (n=4),  
531 and M111A (n=5), with activation effects shown in orange while inhibition effects shown  
532 in blue.

533 **(C and D)** Typical whole-cell current traces and time courses recorded from CHO-K1 cells  
534 overexpressing the TASK-1(V108A) **(C)** or TASK-1(V108A, G105A) **(D)** mutant with 10  $\mu$ M  
535 NPBA.

536 **Figure 4. Segment 131-169 is important for NPBA activation.**

537 **(A-D)** Typical whole-cell current traces and time courses recorded from CHO-K1 cells  
538 overexpressing the T3-240-T1 **(A)**, T3-169-T1 **(B)**, T3-131-T1 **(C)**, or T3-85-T1 **(D)** mutant

**MOL # 115303**

539 channel with 10  $\mu$ M NPBA. Protein secondary structure of chimera is shown beside the  
540 current traces, and section of TASK-3 appears in orange while section of TASK-1 appears  
541 in blue.

542 **(E)** Sequence alignment of TASK-3 and TASK-1 for the residues 131-169. Residues  
543 different in TASK channels appear in jacinth. The TM3 is marked above the sequences.  
544 Residues revealed important in swapping mutagenesis are marked with arrows.

545 **(F)** Typical whole-cell current traces and time courses recorded from CHO-K1 cells  
546 overexpressing the TASK-3(E157A) mutant with 10  $\mu$ M NPBA.

547 **(G)** Histograms summarizing the activation of 10 $\mu$ M NPBA for wild-type TASK-3 and TASK-  
548 3 mutants with substitution of TASK-1 residues within 85-131 or 131-169, with activation  
549 effects shown in orange while inhibition effects shown in blue. A108V is the only mutant  
550 showing a final inhibition with 10 $\mu$ M NPBA. The baseline and NPBA peak-activated current  
551 values and the I/I<sub>0</sub> of TASK-3 mutants was shown in Supplemental Table 1.

552 **Figure 5. Activations by NPBA and chloroform have different**  
553 **determinants.**

554 **(A)** The statistics of the activation of 10 $\mu$ M NPBA for wild-type TASK-3 (n=10), E157Q  
555 (n=4), E157D (n=5), and E157R (n=5). The activation of NPBA on TASK-3 mutants were  
556 compared to wild-type, statistical significance: \* P < 0.05, \*\* P < 0.01, \*\*\* P < 0.001.

**MOL # 115303**

557 **(B)** Typical whole-cell current traces and time courses recorded from CHO-K1 cells  
558 overexpressing TASK-3 channel with 5 mM chloroform.

559 **(C and D)** Typical whole-cell current traces and time courses recorded from CHO-K1 cells  
560 overexpressing the TASK-3(M159W) mutant with 10  $\mu$ M NPBA **(C)** or 5 mM chloroform

561 **(E and F)** Typical whole-cell current traces and time courses recorded from CHO-K1 cells  
562 overexpressing the TASK-3(R245W) mutant with 10  $\mu$ M NPBA **(E)** or 5 mM chloroform

563 **(G and H)** Typical whole-cell current traces and time courses recorded from CHO-K1 cells  
564 overexpressing the 242-3G mutant with 10  $\mu$ M NPBA **(G)** or 5 mM chloroform **(H)**.

565 **(I)** Typical whole-cell current traces and time courses recorded from CHO-K1 cells  
566 overexpressing the A108V mutant with 5 mM chloroform. Magenta trace, current under 5  
567 mM chloroform; blue trace, current under normal bath solution. Period with chloroform  
568 administration is marked by a magenta bar and circle filled with magenta, while circles filled  
569 with blue shown currents with normal bath solution administration.

570 **(J)** Histograms summarizing the activation of 10 $\mu$ M NPBA or 5 mM chloroform for wild-type  
571 TASK-3, M159W, R245W, 242-3G, and A108V, with NPBA effects shown in bars filled with  
572 orange while chloroform shown with bars filled with magenta. n= 4-10.

**MOL # 115303**

573 **Figure 6. A TASK-1 mutant gains the activation by NPBA after A105, A108**  
574 **and E157 transplanted into.**

575 **(A and B)** Typical whole-cell current traces and time courses recorded from CHO-K1 cells  
576 overexpressing TASK-1(V108A, G105A, A157E) **(A)** and TASK-1(V108A, A157E) **(B)**  
577 channel with 10  $\mu$ M NPBA.

578 **(C)** Histograms summarizing the activation of 10 $\mu$ M NPBA TASK-1(V108A, G105A, A157E)  
579 (n=8), TASK-1(V108A, A157E) (n=6) and TASK-1(V108A, G105A) (n=5).

580 **(D)** Important residues for NPBA activation in a topology of TASK-3 subunit.

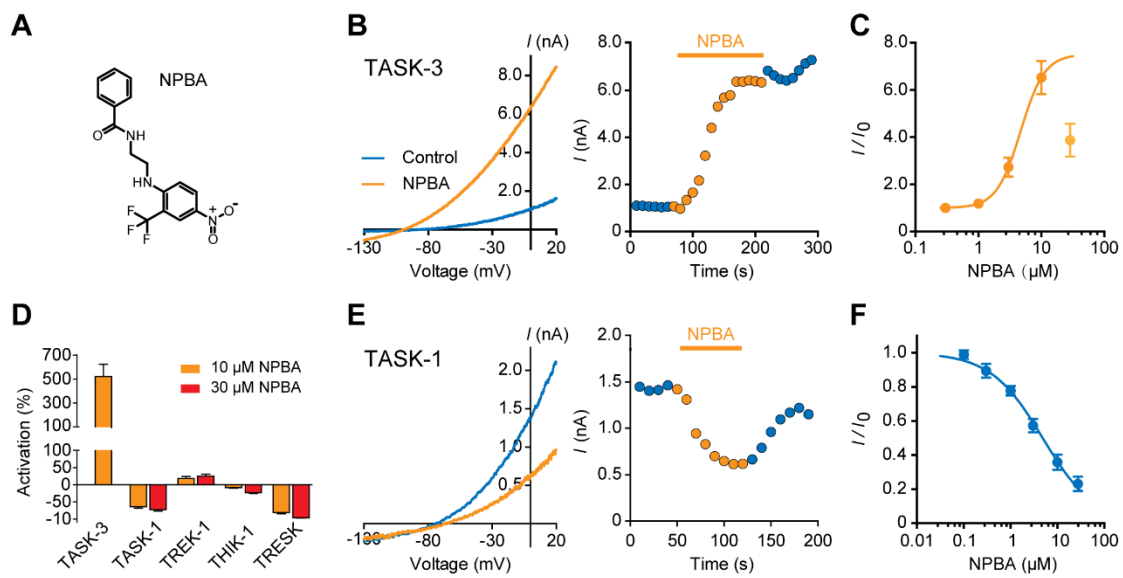
581 **(E)** Homology model of TASK-3 channel. Crucial residues A105, A108 and E157 for NPBA  
582 activation are shown in yellow spheres.

583 **(F)** Top view of TMs and filter domain, the important residues on one TM2 subunit are  
584 labeled.

585 **(G)** Detailed view of protein domains around E157. The putative anesthetic binding pocket  
586 is shown in purple spheres. The up and down states of distal end of TM4 are represented  
587 by TM4<sup>U</sup> and TM4<sup>D</sup> separately.

588 **Figures (6)**

589 **Figure 1**

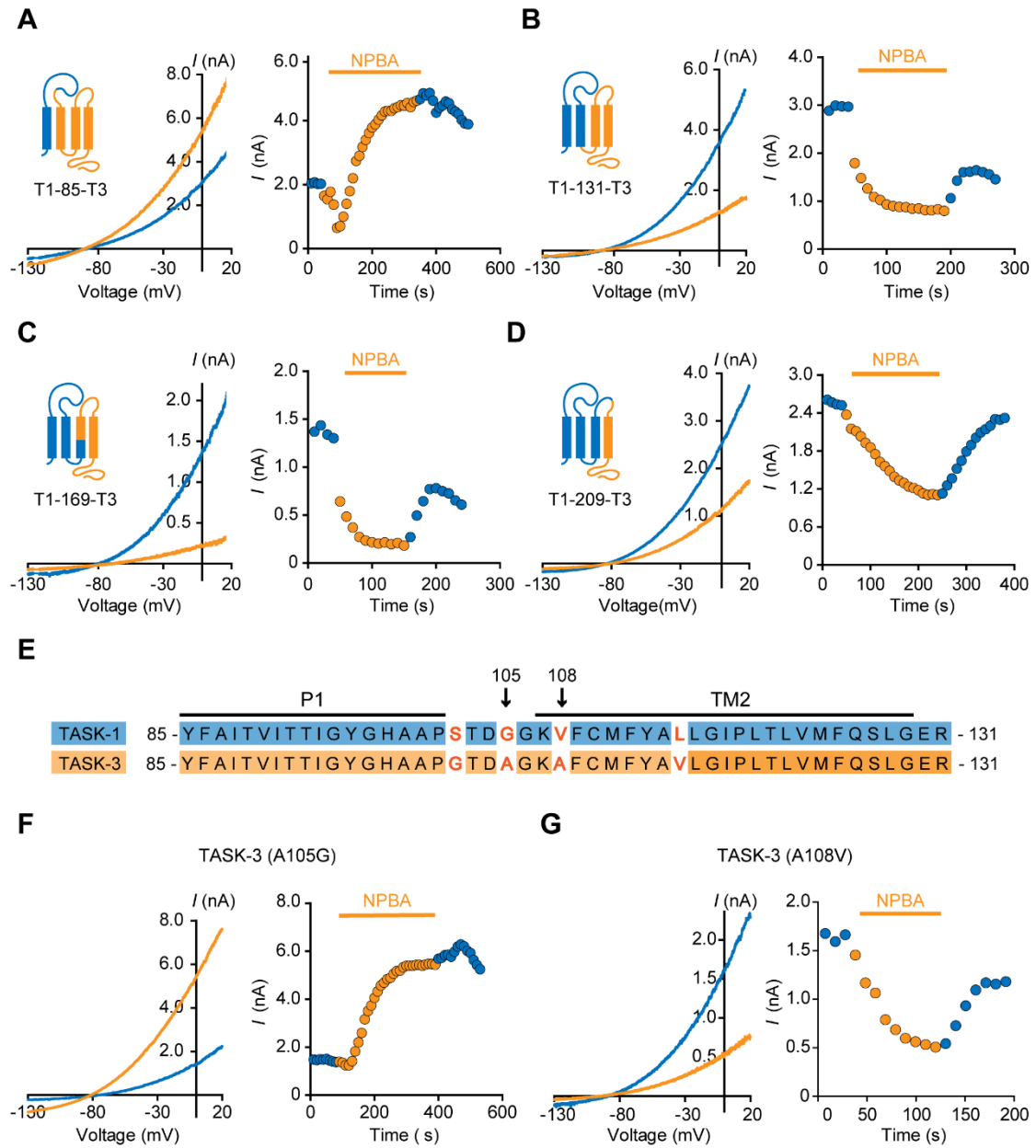


590

591

592

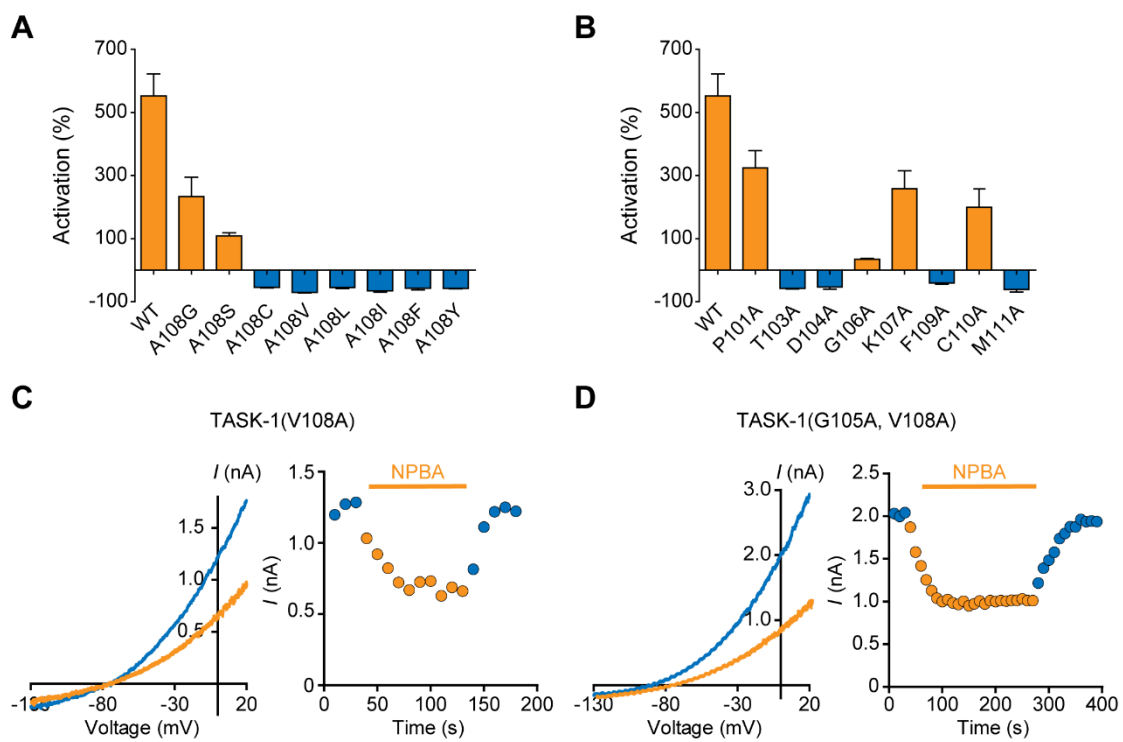
593 Figure 2



594

595

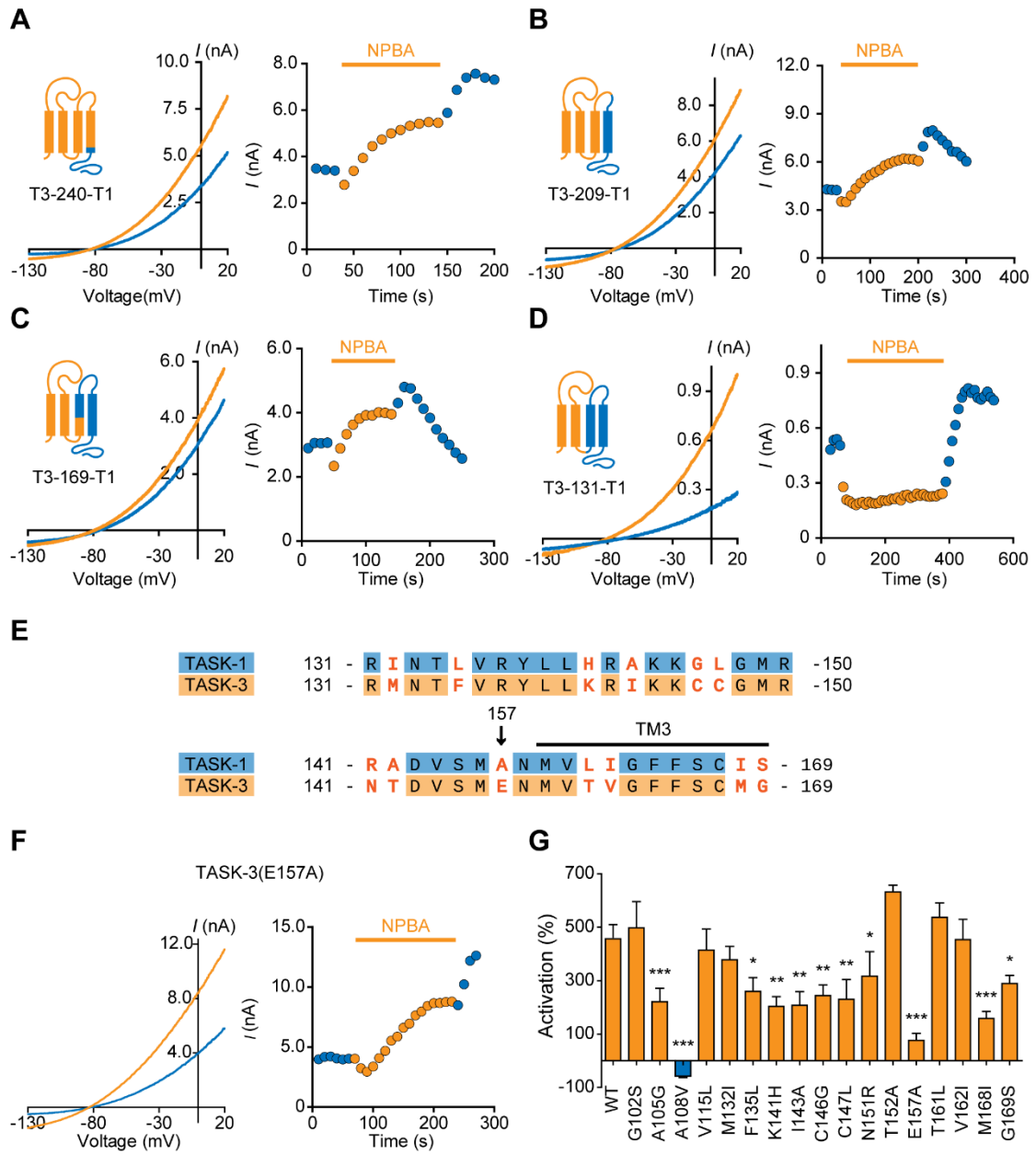
596 **Figure 3**



597

598

599 Figure 4



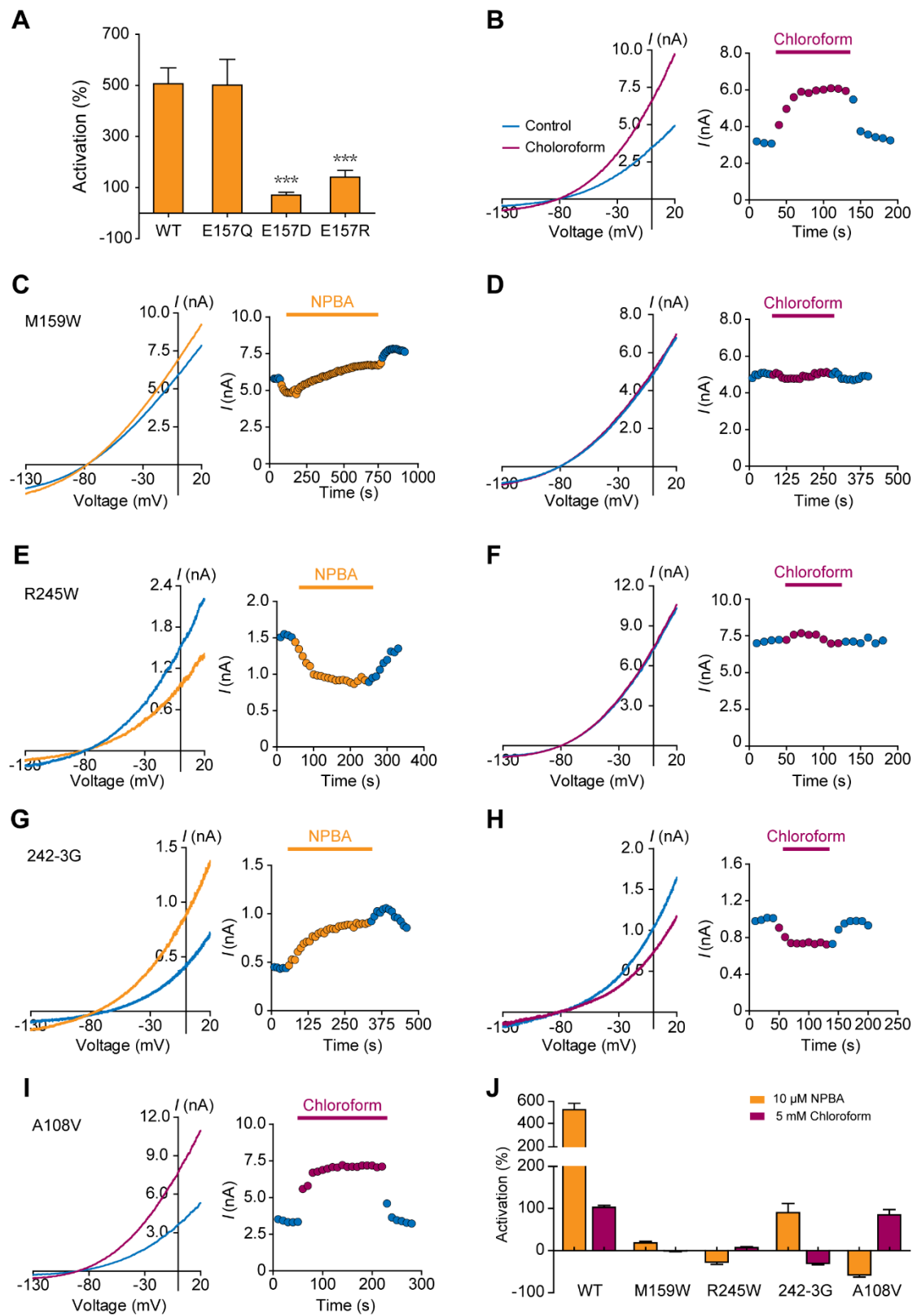
600

601

602

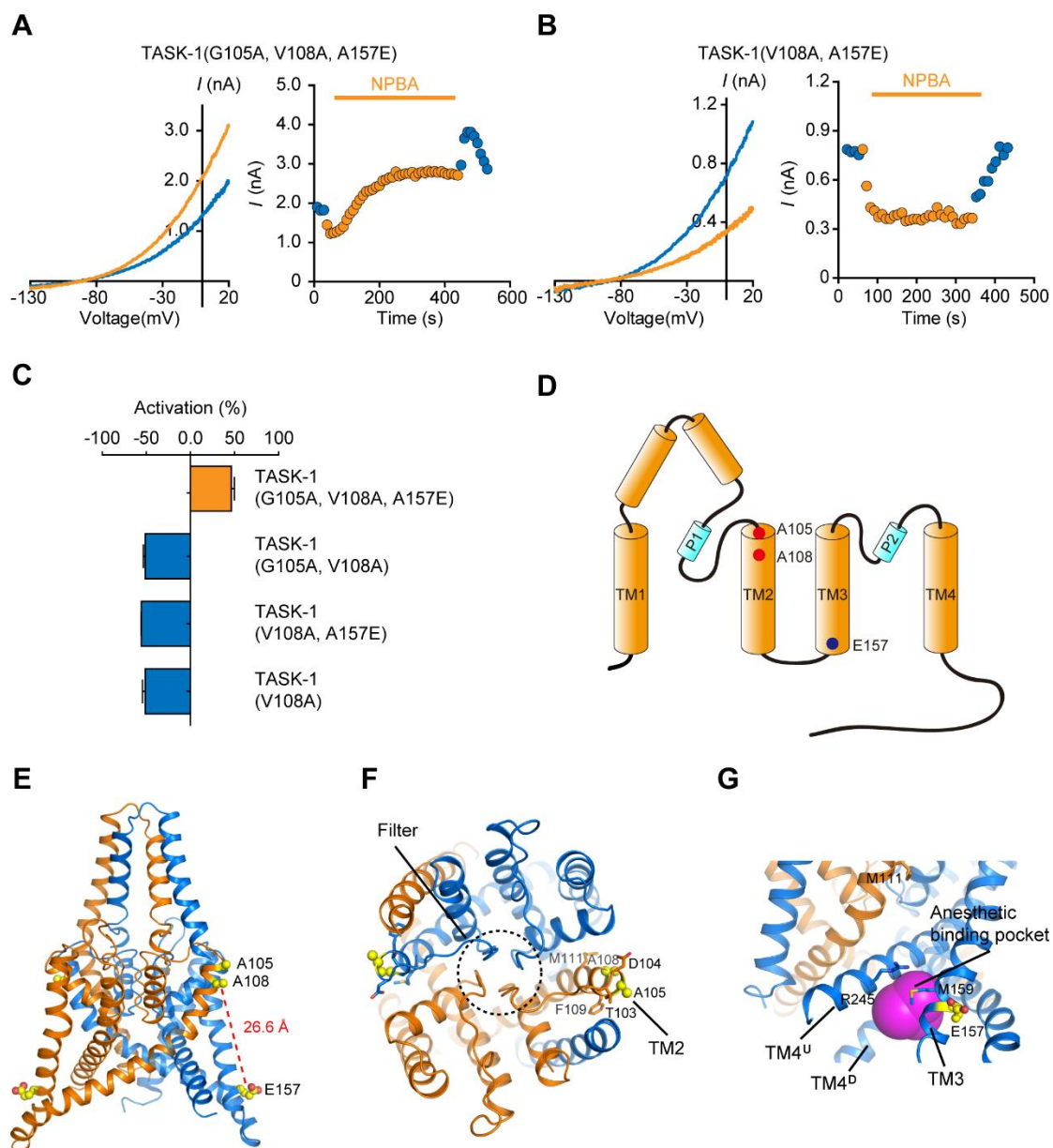


603 Figure 5



604

605 Figure 6



606

607

608

Supplemental Data

**A small-molecule compound selectively activates K2P channel TASK-3 by  
acting at two distant clusters of residues**

Fuyun Tian, Yunguang Qiu, Xi Lan, Min Li, Huaiyu Yang and Zhaobing Gao

Molecular Pharmacology

**Supplemental Table 1.** The baseline and NPBA peak-activated current values and the I/I0

of TASK-3 mutants mentioned in this work. Statistical significance was estimated using

one-way ANOVA followed by Dunnett's post-hoc test, \* P &lt; 0.05, \*\* P &lt; 0.01, \*\*\* P &lt; 0.001.

mutants	baseline current value	peak-activated current value	I/I0
TASK-3 WT	1849.59±447.92	9808.58±1370.21	6.53±0.70
G102S	1909.38±682.67	11096.88±3328.41	5.98±.98
A105G	1669.80±386.34	5690.98±1836.15	3.21±0.51 ***
A108V	3977.61±464.11	1591.49±193.94 **	0.43±0.05 ***
V115L	1526.55±315.65	7627.79±1881.26	5.14±0.79
A108G	2718.±1022.76	7955.7±2193.52	3.33±.62 **
A108S	2840.60±831.54	5915.60±1777.00	2.09±0.10 ***
A108C	876.17±165.90	397.41±74.89	0.45±0.01 ***
A108L	4485.13±1218.78	1959.05±425.15	0.45±0.04 ***
A108I	2945.58±1103.23	917.53±292.79 *	0.35±0.04 ***
A108F	1630.00±275.02	685.00±86.43	0.43±0.05 ***
A108Y	5202.50±1533.89 *	2156.50±600.42	0.42±.01 ***
P101A	630.24±160.72	2030.70±743.54 *	2.96±0.51 ***
T103A	249.56±60.09	141.76±58.09 *	0.45±0.02 ***
D104A	3193.37±521.49	1720.94±344.04 *	0.54±0.05 ***
G106A	1490.27±246.22	2682.82±860.37	1.72±0.26 ***
K107A	277.45±39.15	1082.96±323.12 *	3.59±0.57 ***
F109A	3575.38±725.85	1701.35±382.21	0.46±0.04 ***
C110A	2170.60±804.18	5002.22±1794.91	2.76±0.52 ***
M111A	1283.33±297.05	508.26±111.40 **	0.41±0.05 ***
M132I	2175.02±473.45	10050.53±1809.68	4.78±0.50
F135L	2212.10±901.09	7049.37±2044.47	3.60±0.51 **
K141H	1972.33±693.13	5690.53±2046.22	3.03±0.37 ***
I143A	1745.33±830.99	4932.58±1812.41	3.08±0.51 ***
C146G	1326.40±347.25	4133.78±780.88	3.44±0.39 ***
C147L	1216.95±172.07	3869.54±727.03	3.31±0.74 ***
N151R	1982.78±622.84	6822.34±943.99	4.17±0.92 *
T152A	1351.03±315.14	9824.86±2123.14	7.33±0.25
E157A	2475.30±794.26	4319.80±1439.69	1.82±0.19 ***
T161L	940.67±37.09	5955.46±290.25	6.37±0.54
V162I	5566.40±950.34 **	31009.32±7397.03 ***	5.53±0.76
M168I	2449.75±627.68	6747.08±2260.70	2.58±0.27 ***
G169S	3810.00±1018.15	14904.10±4077.74	3.90±0.30 **
E157Q	1956.53±621.55	11219.92±3873.13	6.01±1.01
E157D	5952.45±811.05 ***	10416.73±2044.36	1.71±0.11 ***
E157R	3366.74±600.23	8852.45±2376.14	2.41±0.26 ***

M159W	4007.86±787.95	4328.85±971.67	1.07±0.07 ***
R245W	6027.15±2651.18 ***	4472.33±1995.53	0.73±0.05 ***
242-3G	313.80±107.47	542.20±188.13	1.91±0.22 ***

---

**Supplemental Figure 1 NPBA activated TASK-3 reversibly.**

(A) Typical whole-cell current traces and time courses with washout phase recorded from CHO-K1 cells overexpressing the TASK-3 with 10  $\mu$ M NPBA.

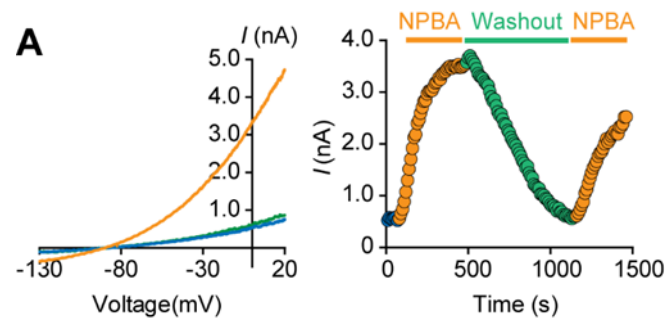
**Supplemental Figure 2 NPBA activation on TASK-3 in presence of chloroform.**

(A) Typical whole-cell current traces and time courses recorded from CHO-K1 cells overexpressing the TASK-3 with 10  $\mu$ M NPBA in the presence of 10 mM chloroform.

(B) The statistics of the activation of 10 $\mu$ M NPBA on wild-type TASK-3, M159W mutant and wild-type TASK-3 in the presence of 10 mM chloroform, statistical significance: \*

$P < 0.05$ , \*\*  $P < 0.01$ , \*\*\*  $P < 0.001$ .

Supplemental Figure 1



Supplemental Figure 2

